Review article

A Review of Laser-Induced Breakdown Spectroscopy (LIBS) for Document Examination: Fundamentals, Mechanism, and Application

Adlina Syafura Ahmad Sabri[1], Hamizah Md Rasid[1], Reena Abd Rashid[1], Umi Kalsum Abdul Karim[2], Mohamed Sazif Mohamed Subri[3] and Mohamed Izzharif Abdul Halim[1]*

[1]*School of Chemistry and Environment, Faculty of Applied Sciences, Universiti Teknologi MARA, 40450 Shah Alam, Selangor, Malaysia*
[2]*Faculty of Applied Sciences, Universiti Teknologi MARA, 35400 Tapah Road, Perak, Malaysia*
[3]*Forensic Laboratory, Criminal Investigation Department, Royal Malaysian Police, 50560 Bukit Aman, Kuala Lumpur, Malaysia*

Curr. Appl. Sci. Technol. 2024, Vol. 24 (No. 3), e0257203; https://doi.org/10.55003/cast.2024.257203

Received: 19 January 2023, Revised: 10 July 2023, Accepted: 10 October 2023, Published: 15 February 2024

Abstract

Keywords

spectroscopy;

laser-induced breakdown spectroscopy;

ink analysis;

document examination;

printing ink;

writing ink

Document examination is one of the main types of investigations in forensic science, particularly in cases involving questioned documents. These documents include assorted forms of written or printed texts on different substrates (paper, banknotes, etc.) with uncertain authenticity. Ink analysis plays a vital role in document examination. It is often focused on understanding the chemical composition of the ink, which can be colorants, solvents, vehicles, and additives. Document examiners utilize several analytical tools including laser-induced breakdown spectroscopy (LIBS). The use of this instrument has gained prominence for its ability to detect multiple elements, offer straightforward sample preparation, minimize sample destruction, and provide fast and accurate readings. This paper reviews previous research that employed LIBS for document examination, highlighting its modern applications and approaches in analysing various types of documents. Furthermore, this paper discusses the strengths and weaknesses of this instrument as a viable technique in the field of document examination.

*Corresponding author: Tel: (+60) 132006530
E-mail: izzharif@uitm.edu.my

1. Introduction

Document examination stands as a key investigation in forensic science. Its primary focus lies in identifying the source of documents and verifying their legitimacy [1]. The growing market for printers, computers, scanners, and photocopiers fuelled the progress of printing technology, which inadvertently promoted the creation of printed document forgeries. Although the use of written documents in the modern age of technology has declined, handwritten signatures and notes continue to be widely utilized by the public as proof of consent [2]. Forged signatures and hand-written alterations on legal documents are still issue in civil and criminal investigations [2, 3]. Therefore, ink analysis of these documents has become indispensable in the field of document examination.

A forensic document examiner (FDE) typically begins the examination of a questioned document by identifying the device used to produce the document (e.g., printers, pens, pencils, etc.), followed by an analysis of the ink's physical properties and chemical composition [4]. Questioned documents refer to any form of written or printed text with questionable authenticity that can be treated as evidence in criminal and/or civil cases [4]. These documents are submitted to forensic document examiners (FDEs) in order to ascertain the authenticity of documents [1]. FDE is responsible for detecting alterations, deletions, and obliterations as well as establishing the exact point in the document's printing time.

Printed documents can be classified based on their printing ink types, such as toner, inkjet, offset, and intaglio. As for writing inks, ballpoint and gel pens are more prevalent in the market compared to rollerball pens, owing to their smoother ink flow and consistent performance [5]. The scope of questioned documents extends beyond ink on paper and encompasses documents with inks on various substrates, including currency bills, identity cards, passports, pharmaceutical packaging, and tax stamps.

Ink, in general, is composed of colorants (dyes or pigments) that are dissolved or suspended in a vehicle (solvent and/or resin) with flowing and drying characteristics [6-8]. This mixture is combined with organic and inorganic additives to impart specific properties, control the ink's density or flowing characteristic, modify the drying process, or influence the ink's actual appearance [8, 9]. Hence, a diverse array of substances, according to the type, brand, and batch of the ink, emit distinct chemical signatures that FDEs can utilize to their advantage [2, 10]. Even though the exact chemical composition of a particular ink is undisclosed by its manufacturers, each ink variant possesses a distinctive fingerprint.

FDE commonly employs visual examinations such as microscopic analysis and light examination with instrumental tools like visual spectral comparator (VSC) [11-13]. However, these techniques are not fool proof and may be subject to human error. The results may be inadequate for the investigation of the authenticity of the documents [12, 13]. Hence, further chemical analysis is necessary to improve the characterization and discrimination of the ink. According to Calcerrada and García-Ruiz [9], numerous analytical approaches (destructive and non-destructive) have their purposes in ink analysis and these approaches have been extensively reported in the scientific literature.

Destructive techniques, despite being time-consuming and requiring delicate sample preparation that eventually damages the sample, are still practiced in forensic analysis. Techniques such as high-performance thin layer chromatography (HPTLC), mass spectrometry, and capillary electrophoresis (CE) offer powerful compound identification of ink components [10, 13, 14]. In contrast, non-destructive techniques require minimal sample preparation with the added advantages of multiple measurements and preservation of the document integrity [15]. These techniques involve utilizing spectroscopy instruments that are occasionally used in tandem and in conjunction with multivariate data analysis. Infrared (IR), Raman, and elemental spectroscopy are a few examples of non-destructive techniques [15-19]. Laser-induced breakdown spectroscopy (LIBS) is also one of

the non-destructive techniques, which falls under laser-based atomic emission spectroscopy and this technique is the central focus of this review.

Brech and Cross [20] first reported the application of LIBS and along the way, LIBS has found its way into other fields of study, such as biology [21-24], geology [25], astronomy [26], archaeology [27, 28], industry [29, 30], and artistic prints [31, 32]. LIBS is a semi-destructive elemental analysis that employs a surface technique using laser ablation with high sample throughput [6, 33-35]. This cost-effective instrument collects information from the ablated mass with high sensitivity and precision [6, 11, 33, 34]. Therefore, this paper discusses the pros and cons of LIBS in document examination by reviewing the results from previous research that employed LIBS. The hybrids of LIBS with other instruments and its role in multivariate data analysis are also discussed.

2. Principle of Laser-Induced Breakdown Spectroscopy (LIBS)

While LIBS is a relatively recent innovation in forensic science, its features, such as lasers, spectrometers, and detectors are constantly being upgraded [33]. Figure 1 shows a typical setup for LIBS, which is compartmentalized into several subsystems as listed below [6, 35-38]:

a) a pulsed laser focused by lenses on the target;
b) a delay pulse generator;
c) an ablation cell for the plasma formation;
d) an optical system to collect emitted signals,
e) a spectrometer with a sensitive detector, and;
f) a computer.

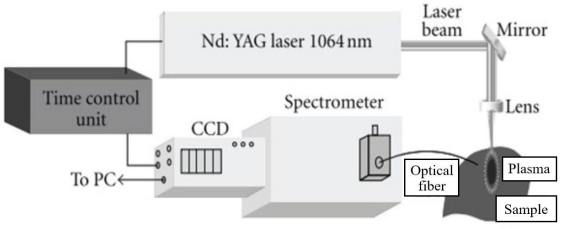

Figure 1. Typical setup of LIBS [39]

The configurations of the spectrometer-detector, laser type, and time control unit as well as environmental factors should be considered to improve any experiment with LIBS [39]. A highly energetic laser-pulsed beam, operating within nanosecond ranges, is directed at the sample surface to induce optical excitation and create plasma [2, 36, 39, 40]. The light energy from the laser beam causes the ablation of a small sample mass, leading to the formation of high-temperature plasma. The temperature at the sample surface rapidly rises to the point of vaporization [37, 39], resulting in various phenomena including photoelectron emission and plasma formation [37]. The plasma parameters such as electron density and excitation temperature contribute to the characteristic transient nature of the laser-produced plasma [41]. The excited atoms and ions of the analyzed sample in the plasma produce distinct lines, bands, and an overlying continuum [2, 37-39]. The main features of these discrete lines are wavelength, intensity, and shape, which aid in sample characterization [2, 39]. Furthermore, the laser energy directly influences plasma emission spectra and the signal-to-noise ratio [42].

In addition to laser energy, laser wavelength plays a crucial role in plasma formation [41]. The appropriate wavelength selection depends on the intended analytical work using LIBS. Moreover, the time delay parameter in LIBS is equally as significant as the laser energy considering the dynamic processes of plasma formation and radiation [42]. The time delay allows for the decay of the continuum radiation before the spectral measurements [38, 42]. The spectra are affected by time variation, wherein the spectrum's formation and the laser plasma's dissipation occur within microseconds (μs) [38]. The process of selecting time delay (gate delay) and integration time (gate window) must be based on the laser wavelength, as it subsequently affects the signal-to-background ratio [39]. An optimized delay time can minimize interferences and improve signal intensity, while a longer time delay may result in lower signal intensities [34, 42].

Plasma emission is directed to a spectrometer using optical fibers and/or lenses [36]. A spectrometer (e.g., Echelle, Czerny-Turner), equipped with a complex optical system, diffracts the collected light, which is then dispersed by a grating, producing “spectral signatures” of the sample [6, 39, 40]. Subsequently, a sensitive detector detects the light, such as a charge-coupled device (CCD), intensified CCD camera (ICCD), silicon CCD (Si-CCD), photodiode array (PDA), or photomultiplier tube (PMT) [6, 39]. Finally, a computer stores and processes the acquired spectrum for further analysis. The spectrum is presented as intensity versus wavelength and the spectral lines are attributed to elements present in the samples [33]. The spectral lines are typically shown in the range of 190 nm to 900 nm. The wavelengths can be compared to the database of the National Institute of Standards and Technology (NIST) [6, 33, 43, 44]. Additionally, simultaneous quantification is also possible, where the concentration of the elements can be determined based on their emission intensity [6].

Optimizing the parameters for LIBS measurements requires a comprehensive understanding of LIBS plasma physics and consideration of environmental factors that may affect the plasma lifetime and features [39]. The plasma lifetime stages are depicted in Figures 2(a) and 2(b) [39, 45]. Figure 2(a) presents an overview of the plasma lifetime, which is divided into three stages (labelled as i, ii, and iii), whereas Figure 2(b) provides a more detailed explanation of each stage, appropriately labelled with the corresponding stages. When the laser induces the creation of plasma (Figure 2(a-i)), several processes take place, beginning with the emission of continuous Bremsstrahlung [37, 41].

The first stage is ignition which involves breaking the bond and plasma shielding during the laser pulse. When the laser interacts with matter, photons are absorbed by atoms, causing the transition of electrons to higher energy levels (Figure 2(b-i) in laser energy absorption) [39]. This process depends on laser type, duration of the laser pulse, and irradiance. The plasma shielding effect occurs when the plasma becomes opaque for the last part of laser radiation. At this stage, the plasma surface absorbs or reflects the laser pulse, preventing the ionization of the material and reducing the ablation rate as the radiation does not reach the sample surface. Consequently, craters with melted and deposited material are formed. Simultaneously, the plasma is reheated, which multiplies the lifetime and size of the plasma, as displayed in Figure 2(a-ii) where the plasma has enlarged in size. This stage only lasts for a few ns to a few μs.

The second stage is plasma expansion and cooling, which is influenced by factors such as ablated mass, spot size, energy coupled to the sample, and environmental conditions [39]. This process is crucial for optimizing LIBS spectral acquisition since atomic emission occurs during the cooling process. Furthermore, the recombination of electrons and ions in this stage is essential for generating line emission, which impacts the radiation processes [41].

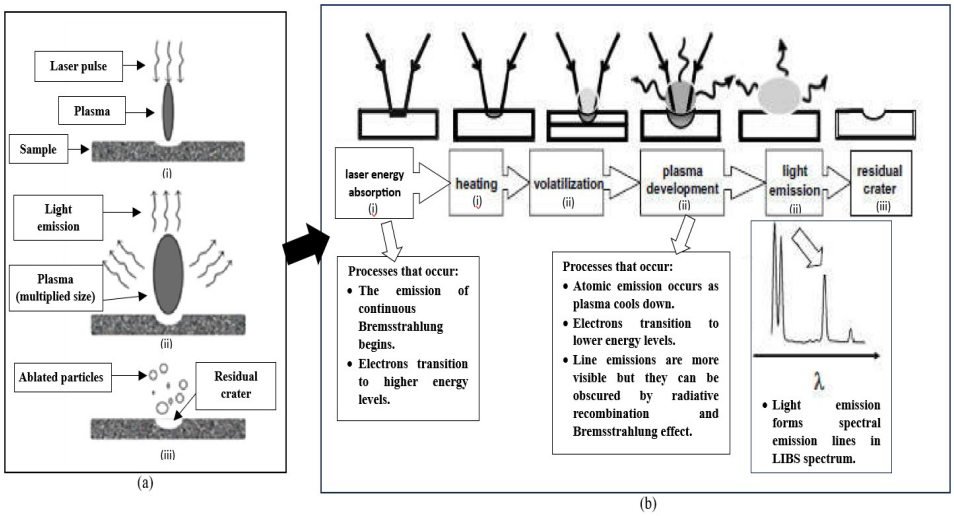

Figure 2. Schematic diagram of plasma lifetime stages; (a) an overview of plasma lifetime stages (i, ii, and iii) and (b) detailed explanation of these stages [39, 45]

As the plasma continues to expand and cool after ignition, there is a concurrent change in electron temperature and density. During this process, electrons transition to lower energy levels and the electrons emits photons in the decay. This process is synonymous with the de-excitation of atoms [39]. Line emissions become more visible as the plasma cools down after plasma formation (Figure 2(b-ii) in plasma development). However, these line emissions can be obscured by the continuous emission due to radiative recombination and the Bremsstrahlung effect [37, 39]. Initially, the plasma radiation appears as a continuous spectrum that diminishes rapidly as the plasma relaxes [37, 41]. This plasma radiation constitutes atomic lines from the decay of excited atoms, ions, and small molecules [37, 41].

The distinct energy levels of different atoms cause them to emit characteristic photon energies with narrowband emissions, forming the spectral emission lines in the LIBS spectra as illustrated in Figure 2(b-ii) (in light emission). Therefore, a time delay in the time control unit is necessary to avoid the continuum radiation, as previously explained [37, 39]. The second stage occurs within a few microseconds to a few milliseconds. The final stage of the plasma lifetime involves particle ejection and condensation, which do not affect LIBS measurements [39]. Some of the mass is ablated as particles that create condensed vapor, liquid sample ejection, and solid sample exfoliation (Figure 2(a-iii)). This stage can last from milliseconds to several seconds.

3. Instrumental Setup in Laser-Induced Breakdown Spectroscopy (LIBS)

The setup of LIBS involves selecting the best laser source as the light energy and the configuration of laser parameters such as wavelength, pulse time, and laser energy. Optimization and calibration of LIBS parameters are imperative to acquire the highest intensity of signals without saturating the spectrum [34, 46]. Previous research's instrumental setup and parameters of LIBS for document examination are summarized in Table 1.

Table 1. Parameter setup of LIBS for document examination

Sample	Laser Source	Spectrometer	Time Delay	Detector	Spot Size	Additional Notes	Ref.
Ballpoint, gel, porous point, and rollerball ink pens on paper	• Type: Nd:YAG • Wavelength: 1064 nm • Energy: 150 mJ	Czerny-Turner (255-416 and 496-718 nm ranges)	165 µs	CCD	Not available	• The detector was fixed with 1.27 µs of fixed gate delay and 1.2 ms of integration time. • Spectral resolution was 0.1 nm. • The experiment was performed in ambient air using scan mode.	[2]
Ballpoint and gel ink pens on paper	• Type: Nd:YAG • Wavelength: 1064 nm • Energy: 30 mJ (for 6.5 ns	Four compact spectrometers (200-795 nm ranges)	0.5 µs	Not available	Not available	• Laser pulses were repeated ten times with a repetition rate of 2 Hz. • A 1-m fiber bundle with four 600 µm diameter quartz fibers was used to direct the light to the spectrometers. • Spectral resolutions were varied for different wavelength intervals. • The minimum acquisition gate was set at 1.05 ms.	[3]
Gel ink pens on paper	• Type: Nd:YAG • Wavelength: 1064 nm • Energy: ~87 mJ (for 5 ns)	Echelle	Not available	ICCD camera	Not available	• 1.5 mm optical fiber with 600 µm diameter was used.	[4]
Ballpoint ink pens on paper	• Type: Frequency-doubled pulsed Nd:YAG • Wavelength: 532 nm • Energy: 200 mJ (for 7 ns)	Echelle (equipped with the individual optical system and entrance slit aperture in the range of 290-930 nm)	Not available	CCD camera	Not available	• The LIBS system was integrated with Raman spectroscopy, and the spectra of both LIBS and Raman were randomly fused to maintain the variance of both data sets.	[7, 47]

Table 1. Parameter setup of LIBS for document examination (continued)

Sample	Laser Source	Spectrometer	Time Delay	Detector	Spot Size	Additional Notes	Ref.
Ballpoint and gel ink pens on paper	• Type: Nd:YAG • Wavelength: 1064 nm • Energy: 50 mJ	Czerny Turner spectrograph	1.4 µs	ICCD	~450 µm	• The ablation mode used was line mode. • Scan rate was set at 50 µm / 2 s. • Laser pulse was repeated at 2 Hz rate for 100 shots and the gate width was set at 4 µs.	[11]
Ballpoint ink pens on paper	• Type: Nd:YAG • Wavelength: 1064 nm (spectra acquired at 186-1042 nm ranges) • Energy: 78 mJ	Not available	1.64 ms	Not available	50 µm	• Three laser pulses were used for each point during LIBS measurement. • Inductively Coupled Plasma Optical Emission Spectroscopy (ICP OES) was used for confirmatory evaluations.	[48]
Ballpoint and gel ink pens on paper	• Type: Nd:YAG • Wavelength: 1064 nm (spectra collected at 200-900 nm ranges) • Energy: Varied energies ranging from 60-500 mJ	Not available	Not available	Si-CCD array	Not available	• Optical fiber with a 200 µm diameter was used. • The integration time was set at 500 ms.	[49]
Gel ink pens on paper	• Type: Nd:YAG • Wavelength: 1064 nm (IR) and 532 nm (visible) • Energy: ~25 and ~87 mJ (IR) and ~25 mJ (visible)	Echelle spectrometer	Not available	ICCD camera	Not available	• A 1.5 m optical fiber with 600 µm diameter was used.	[47]
Inkjet and toner inks on paper	• Type: Nd:YAG • Wavelength: 1064 nm (spectra acquired at 173-956 nm) • Energy: 120 mJ (for 10 ns)	Not available	Not available	CCD	Not available	• A 200 µm-diameter optical fiber was used.	[45]

Table 1. Parameter setup of LIBS for document examination (continued)

Sample	Laser Source	Spectrometer	Time Delay	Detector	Spot Size	Additional Notes	Ref.
Toner and inkjet inks on paper	• Type: Nd:YAG • Wavelength: 1064 nm • Energy: 270 mJ (for 10 ns)	Ocean Optics HR4000 spectrometer	Not available	Not available	Not available	• Laser voltage was set to 900 mJ with an integration time of 100 ms. • 60 µm UV-Vis optic fiber was used. • The experiment was performed in ambient air.	[46]
Toner and inkjet inks on paper	• Type: Nd:YAG • Wavelength: 1064 nm • Energy: 170 mJ	Ocean Optics LIBS2500+ spectrometer	2.6 µs	Not available	300 µm	• Sample chamber was first purged with argon gas for 60 s to remove air and to augment spectral intensity. • The analysis mode was line mode.	[50]
Toner and inkjet inks on paper	• Type: Nd:YAG • Wavelength: 1064 nm • Energy: Not available	6-channel broadband spectrograph (190 -1040 nm)	1.4 µs (inkjet) & 1.2 µs (toner)	CCD linear array	300 µm	• Integration time was fixed at 1.1 ms. • Optimum parameters were at 35% energy for 150 shots at 2 Hz frequency and 25 µm/s speed rate.	[51]
Toner ink on paper	• Type: Nd:GGG • Wavelength: 198-318 nm (UV ranges) & 345-888 nm (Vis ranges) • Energy: 10 mJ	Two-channel fiber optic spectrometer	40 µs (double-pulse mode)	CCD	Not available	• The laser was set up for two consecutive pulses with equal energy. • Integration time was 2 ms. • The measurements were performed under argon gas.	[52]
Toner, inkjet, intaglio, and offset inks on paper	• Type: Nd:YAG • Wavelength: 1064 nm • Energy: 7.8 mJ (inkjet), 13 mJ (toner), 4.1 mJ (offset & intaglio)	6-channel-broadband spectrometer of 190-1040 nm	0.1 µs (inkjet, offset & intaglio) & 0.8 µs (toner)	CCD linear array	200 µm	• LIBS was used in tandem with Laser Ablation – Inductively Coupled Plasma – Mass Spectrometry (LA-ICP-MS). • The ablation mode was single line mode.	[53]

Table 1. Parameters setup of LIBS for document examination (continued)

Sample	Laser Source	Spectrometer	Time Delay	Detector	Spot Size	Additional Notes	Ref.
Pencil marks	• Type: Nd:YAG • Wavelength: 1064 nm • Energy: 60 mJ (for 10 ns)	Not available	1.5 µs	Not available	100 µm	• A coupling fiber was used to direct the signal from plasma emission into the LIBS spectrometer.	[1]
Ink on banknote papers	• Type: Nd:YAG; • Wavelength: 1064 nm (spectra collected at 185-904 nm UV-Vis ranges); • Energy: 150 mJ (for 6ns)	6-channel Czerny-Turner	Not available	CCD	Ranged from 0.6 to 1 mm	• The experiment was performed at atmospheric pressure in the air. • The spectral resolution was around 0.1 nm.	[34]
Ink on pharmaceutical packages	• Type: Nd:YAG • Wavelength: 266 nm • Energy: 5.4 mJ	6-channel Czerny-Turner (190-1040 nm ranges)	0.9 µs	Not available	100 µm	• The ablation mode used a straight-line mode.	[40]
Passports and identity cards	• Type: Nd:YAG • Wavelength: 1064 nm • Energy: 150 mJ (for 6 ns)	6-channel Czerny-Turner (185-904 nm ranges)	Not available	CCD	0.4-0.8 mm	• The detector was fixed with gate delay of 1.27 µs and integration time of 1.5 ms. • Spectral resolution was set at around 0.1 nm. • The experiment was performed under atmospheric air pressure.	[54]
Tax stamps	• Type: Nd:YLF • Wavelength: 1053 nm • Energy: 600 µJ (for 470 ps)	Czerny-Turner polychromator (200-850 nm ranges)	Not available	CCD sensor array	80 µm	• Optical fibre with a 100 µm core cable was used. • The laser pulse was set with 100 Hz repetition rate.	[55]

As seen in Table 1, most studies utilized Nd:YAG laser as the light source with a wavelength of 1064 nm despite the type of documents. Nd:YAG laser with a fundamental mode of 1064 nm was the preferred laser for LIBS as it could quickly generate compact plasma [39]. As highlighted by Anabitarte *et al*. [39], a higher laser wavelength produced a lower ablation rate with a higher elemental fractionation.

Elsherbiny and Nassef [47] conducted LIBS study using both visible and IR lasers as excitation sources with fundamental wavelengths of 1064 nm and 532 nm, respectively. The pulse energies of these lasers were also varied for each wavelength as stated in Table 1. One study switched the light source to Nd:GGG laser with a wavelength range of 198 nm to 888 nm (UV-Vis ranges) [52]. The change in the light source was motivated by the conversion to a micro-LIBS system. The authors also configured the laser to emit two consecutive pulses to increase the intensities of LIBS signal emission. Another study utilized Nd:YLF laser for tax stamp samples with a wavelength of 1053 nm as shown in Table 1, and this laser type used the lowest laser energy (600 μJ) compared to the other types [55].

Several researchers used Czerny-Turner [2, 11, 34, 40, 54, 55], Echelle [4, 7, 47] and Ocean Optics [46, 50] spectrometers in their studies. Czerny-Turner spectrometer is commonly used in LIBS. The spectrometer has an entrance slit, two mirrors, and a diffraction grating [39]. Light passes through the slit and collides with the first mirror, which pivots the light onto the grating. Then, the second mirror focuses the light onto the focal plane with the detector. The choice of detectors depends on the application of the instrument.

According to Table 1, some researchers used various types of CCD detectors for document examination, while others did not divulge details of the type of detector. CCD detectors provide less background signal for two-dimensional spatial information [39]. The spot size and laser pulse energy determine the fluence, which is the amount of energy per area [48]. Large spot size increases the number of pulses delivered in a small area, which enhances the resolution of chemical images. Several researchers measured the spot size, and it was larger for banknote papers (0.6 mm to 1.0 mm) [34] and identity documents (0.4 mm to 0.8 mm) [54] compared to ink on paper samples (~50 μm to ~450 μm). All studies kept the spectral resolution constant, except for a study by Cicconi *et al*. [3], where they varied the values according to the intervals of wavelength (0.07, 0.09, 0.10, and 0.16 nm for 200-270 nm, 270-400 nm, 400-546 nm, and 570-795 nm, respectively).

Hilario *et al*. [48] applied ICP OES in conjunction with LIBS for confirmatory evaluation of the differentiation of the ballpoint ink pens. ICP OES was performed in robust conditions using argon gas (99.999%) for plasma generation and maintenance in the instrument. A combination of LIBS and Raman was applied by Hoehse *et al*. [7] to examine ballpoint ink pens on paper. The researchers previously published an extensive article on the instrumental setup of this combination for elemental and molecular microanalysis [47]. A mechanical chopper was employed in the instrument to cut off an initial plasma continuum in order to prevent the CCD from detecting early continuum radiation from LIBS plasma [7, 47]. The spectra acquired from LIBS were randomly fused with Raman spectra to maintain the variance of both data sets. For instance, LIBS spectra from 2432 cm^{-1} to 1797 cm^{-1} were attached to Raman spectra from 1796 cm^{-1} to 300 cm^{-1}.

Subedi *et al*. [53] explored the application of tandem LIBS with laser ablation – inductively coupled plasma–mass spectrometry (LA-ICP-MS). A fiber optic collected the excitation of samples by the emitted light in the LIBS plasma to a CCD spectrometer. An argon carrier gas transported the ablated particles to the inductively coupled plasma (ICP). Moreover, the researchers varied the laser energy and frequency according to the ink type [53]. The highest energy was used for inkjet ink (13 mJ). Additionally, laser frequency was varied according to ink type. A higher frequency was used for toner ink (1.8 Hz), offset ink (4 Hz), and intaglio ink (4 Hz) compared to inkjet ink (0.8 Hz) [53]. High frequency can cause more damage to the samples. Therefore, low frequency is more suitable for inkjet ink to minimize interferences from paper since the ink is immersed in the paper.

4. Elemental Analysis

LIBS can perform qualitative and quantitative chemical analyses at the atomic level, with several strengths and limitations [39]. A summary of the advantages and disadvantages of LIBS in document examination is presented in Table 2. Qualitative analysis can be carried out accurately using LIBS as it detects the atomic emission of all elements in the analyzed sample [39]. Quantitative analysis of LIBS determines the relative amount of elements in units of ppm (concentration of elements), ng (absolute mass of elements), or ng/cm^2 (surface concentration) [39]. This analysis encompasses the non-calibration method and calibration method. The latter uses a calibration curve tied to experimental factors [39, 56].

Table 2. Advantages and disadvantages of LIBS for document examination

Advantages	Disadvantages
• LIBS is capable of simultaneous rapid multi-elemental detection (<1 second per analysis) in ink samples [34-36, 38, 51, 57]. • LIBS can analyze any ink material, irrespective of its physical states (solid, liquid, gas, etc.) [38, 42, 57]. • LIBS can properly identify each emission line for a specific element in a neutral or ionized state [39]. • There is no requirement to prepare or treat the ink samples prior to analysis of LIBS [2, 38]. • LIBS does not require pre-set elemental menu as in LA-ICP-MS [51, 53]. • LIBS can provide inorganic information about the printing ink which is a rare feature in standard techniques [52].	• The optimization and development of LIBS are time-consuming [50]. • LIBS may not be sensitive enough in the quantitative analysis compared to other atomic emission spectroscopies [38]. • There can be spectral noise due to the presence or absence of distinct emission lines that interfere with elemental analysis [34]. • It is difficult to interpret a large volume of data from LIBS with many variables in a short period [33, 46]. • LIBS is a semi-destructive instrument, leaving a small visible crater after the laser ablation [2, 11, 35, 46].

According to Table 2, LIBS does not require any sample pretreatment, which is favorable for ink samples as the sample integrity can be preserved [2, 38]. In addition, broadband scanning can be employed by LIBS to detect unusual peaks without requiring a pre-set elemental menu, unlike in LA-ICP-MS [51, 53]. Table 2 also presents the limitations of LIBS in analysis of various types of ink. Elemental analysis using LIBS may be affected by spectral noise. However, this issue can be resolved by selecting valid spectral lines to generate reproducible spectra with consistent qualitative differences in the samples [34]. Another issue the researchers faced was difficulty in interpreting multivariable data from LIBS, and thus a reliable overall data analysis could not be achieved [33, 46]. Nevertheless, statistical analysis was applied for a systematic classification and differentiation of the samples.

Certain elements were not listed by researchers in their studies due to many factors. Lennard *et al*. [50] rejected the analysis of several elements due to poor precision (low relative standard

deviation) and the fact that their concentrations were below the detection limits. On the other hand, Hui *et al*. [46] selected a few regions of interest in order to minimize the effect of the paper spectrum, and thus certain elements were discarded from the list of elements reported in their study. Trejos *et al*. [51] facilitated the use of signal-to-noise ratio (SNR) in the selection of elements. Additionally, certain elements such as S and I were rejected by the researchers due to the limited ability of suitable standards. Elements found by Król *et al*. [34] with low-intensity signals were not accepted as significant spectral lines. Furthermore, the researchers did not list several elements that exhibited many intense lines as these elements were not categorized as persistent in the NIST database.

Metzinger *et al*. [52] microscopically scrutinised the images of before and after LIBS analysis on inkjet and toner ink on paper to measure the size of the craters. They observed that the diameters of all craters after ablation were tenfold or a hundredfold larger than the microspot size for all prints, which was only a few µm in diameter. Deep craters of 30 µm to 95 µm in diameter were observed for inkjet ink. The low-density fibrous structure of the paper caused higher penetration of laser on inkjet ink. For toner ink, the ablation only affected the toner layer, which was caused by the strong absorption of light energy in the layer. The toner particles had a weak adhesion to the paper fibre, and their heat conduction was higher than the materials in the paper.

Additionally, Król *et al*. [54] measured the diameter of the craters on samples of identity documents with 400 µm to 800 µm. Due to the resultant craters after laser ablation, the size of the craters should be taken into account to ensure the least amount of ablated substrate on which the ink was deposited. Despite these disadvantages, several researchers argued that LIBS was a viable technique to distinguish printing ink from various sources [46, 51].

4.1 Detected elements in hand-written documents

Comparative analysis of writing instruments benefits from the various combinations of colorants that are present in the inks [2]. Most studies focused on ballpoint pens as sample subjects. Gel pens have gained popularity since the late 1990s [5], however, to date, only three studies of these pens using LIBS to distinguish the inks from various sources have been conducted [2, 11, 47]. Future research should be concentrated on analyzing gel pens due to their wide availability in the market. Table 3 listed the elements reported in previous studies that were found in hand-written documents. However, a study by Sadam *et al*. [49] did not specify the pen type (i.e., ballpoint and gel pens) for the elements they reported. As highlighted by Lennard *et al*. [50], ink analysis is more challenging compared to the analysis of paper. The difficulty lies in isolating the pen inks from the substrate since these inks are absorbed into the paper fibers.

As seen in Table 3, Cu and Mn were detected in all studies involving gel pens and several authors also discovered Cr [2, 47] and Mg [11, 47]. As for ballpoint pens, most studies observed the presence of Cr and Mn. Other common elements found in these pens were Ba [2, 48, 50], Cu [2, 3, 48], Li [2, 7, 50], and Ni [2, 3, 50]. Lennard *et al*. [50] noted the presence of Mg I, Si I, Al I, Ti II, Ca I, and Na I at 285.21 nm, 288.21 nm, 308.22 nm, 336.12 nm, 643.91 nm, and 819.48 nm, respectively in ballpoint pens. In a study conducted by Hilario *et al*. [48], a scores map was constructed by selecting sample signals from ballpoint pens that were greater than paper signals, namely Ca (392-395 nm and 315-319 nm), Cr (396-398 nm and 422-423 nm), Mn (247.5-248.5 nm), Ti (279-281 nm), and Cu (520-522.5 nm).

Several researchers classified the pen samples based on their colors [2, 3]. Kula *et al*. [2] categorized pen inks according to both their type (ballpoint, gel, rollerball, and porous-point) and color (blue, black, and red). The differences in the elemental profile of the pens according to their types are shown in Table 3. Similar elements such as Cu (324.7 nm, 327.4 nm, 510.6 nm, 515.3 nm, and 521.8 nm), Cr (~360 nm and ~520.5 nm), Li (670.7 nm), and Mn (~403 nm) were observed in all three colors. Cu was characteristic of blue inks, while black inks did not exhibit any characteristic

element. Blue inks contained additional elements Ni, Ba, and W. Red inks had the highest number of indistinguishable samples, mainly due to the use of cationic dyes (e.g., Rhodamine B). The researchers highlighted that Li is preferred as a counterion for anionic dyes compared to Na and K. Additionally, they determined the discrimination power by calculating the ratio of successfully differentiated ink pairs to all possible ink pairs of the same color. Based on these calculations, ballpoint and gel pens showed similar values of discrimination power. The discrimination power was higher for blue and black inks compared to red inks.

As seen in Table 3, the presence of Cu was observed in several studies related to ballpoint pens [2, 3, 47]. Figure 3 shows several spectra that detected the presence of Cu in ballpoint pens. Cicconi *et al*. [3] pointed out that blue pens commonly contain phthalocyanine blue BN, where Cu is coordinated inside the phthalocyanine ring. Black inks, on the other hand, may consist of a black pigment or a combination of various colorants such as violet, blue, yellow, and red. Nigrosine, with its main structural unit as phenazine, can also be present in black inks. Black dyes are produced by heating a mixture of nitrobenzene, aniline, and hydrochloric acid with Cu or Fe. Other than ballpoint and gel pens, Kula *et al*. [2] analyzed rollerball and porous-point pens. They detected similar elements of Cr, Mn, and Li in both pen types. Trejos *et al*. [11] conducted both qualitative and quantitative comparisons of gel pen samples. They selected Cu I (324.3 nm), Na I (330.2 nm), Mg II (280.2 nm), and Mn II (255.8 nm) for quantitative differentiation. Additional lines of these elements were used for qualitative comparisons.

Sadam *et al*. [49] optimized the LIBS setup by increasing laser energy from 60 mJ to 80 mJ which resulted in an increase in the power density. The increase in power density had a positive effect on the intensities of emission lines as it produced a higher mass ablation rate, leading to an increased number of excited atoms and intensities of spectral lines. However, it was noted that excessively high-power density increased the influence of the paper's spectrum which potentially interfered with the ink analysis. Elsherbiny and Nassef [41] tested different wavelengths and energies of the laser pulse. They observed that different wavelengths produced different spectra. When using a 1064 nm-wavelength IR laser pulse, several spectra did not display any characteristic emission lines after subtracting the paper's spectrum, which could not differentiate the gel ink samples. This was because the IR laser was well-absorbed by the black ink, resulting in insufficient laser energy being available to produce characteristic atomic or ionic lines from the samples.

To address this issue, the researchers increased the laser pulse energy while being careful not to damage the samples. No significant differences were observed for ink samples from the same sources. Nevertheless, ink samples from different sources were successfully distinguished using this approach. Chen *et al*. [1] conducted an analysis of pencil marks and discovered that chemical components in all four analyzed samples were similar, as can be seen in Table 3 (i.e., C, Mg, Al, Ca, Si, and Fe). The researchers noted that due to the similar composition of the samples, it was challenging to differentiate the pencil marks based solely on the spectrum. Thus, further analysis using machine learning methods was necessary to effectively distinguish these samples.

4.2 Detected elements in printed documents

The elemental composition of a printing ink can vary due to the addition of additives, driers, pigments and/or dyes during its manufacture [51]. Qualitative and semi-quantitative data from peak intensities are favored over complete quantitative methods when comparing the toner and inkjet samples. Table 4 shows a list of elements detected in previous studies. Most studies provide detailed information on ink types, except the study by Hui *et al*. [46]. The most analyzed ink types were toner

Table 3. List of elements detected in hand-written documents

Sample	Elements													Ref.
	Ba	**Cr**	**Cu**	**Fe**	**Li**	**Mn**	**Mo**	**Ni**	**W**	**Zr**	**Ca**	**Ti**	**K**	
Ballpoint ink pens	/	/	/	/	/	/	/	/	/	×	×	×	×	[2]
	×	/	/	/	×	/	×	/	×	×	×	×	×	[3]
	×	×	×	×	/	×	×	×	×	×	/	×	/	[7]
	/	/	/	×	×	/	×	×	×	×	/	/	×	[48]
	/	/	×	/	/	/	/	/	/	×	×	×	/	[50]
Ballpoint and gel ink pens	×	/	/	/	×	×	×	×	×	×	/	/	×	[49]
Gel ink pens	×	/	/	/	/	/	×	×	×	×	×	×	×	[2]
	×	×	/	×	×	/	×	×	×	×	×	×	×	[11]
	×	/	/	×	×	/	×	/	×	×	×	×	×	[47]
Rollerball ink pens	×	/	×	×	/	/	×	×	×	×	×	×	×	[2]
Porous-point ink pens	×	/	×	×	/	×	×	×	×	×	×	×	×	[2]
Pencil marks	×	×	×	/	×	×	×	×	×	×	/	×	×	[1]

/ indicates the presence of the element in the sample.
× indicates the element was not reported by the authors.

Table 3. List of elements detected in hand-written documents (continued)

Sample	Elements													Ref.
	Mg	**V**	**Cd**	**Al**	**La**	**P**	**Zn**	**Pb**	**Si**	**Co**	**S**	**Ta**	**Na**	
Ballpoint ink pens	×	×	×	×	×	×	×	×	×	×	×	×	×	[2]
	×	×	×	×	×	×	/	/	×	×	×	×	×	[3]
	×	×	×	/	×	×	×	×	×	×	×	×	/	[7]
	×	×	×	×	×	×	×	×	×	×	×	×	×	[48]
	×	×	×	/	×	×	×	×	×	×	×	×	×	[50]
Ballpoint and gel ink pens	/	/	×	/	×	/	×	×	/	/	/	/	/	[49]
Gel ink pens	×	×	×	×	×	×	×	×	×	×	×	×	×	[2]
	/	×	×	×	×	×	×	×	×	×	×	×	/	[11]
	/	×	×	×	×	×	×	×	/	×	×	×	×	[47]
Rollerball ink pens	×	×	×	×	×	×	×	×	×	×	×	×	×	[2]
Porous point ink pens	×	×	×	×	×	×	×	×	×	×	×	×	×	[2]
Pencil marks	/	×	×	/	×	×	×	×	/	×	×	×	×	[1]

/ indicates the presence of the element in the sample.
× indicates the element was not reported by the authors.

Table 4. List of elements detected in printed documents

Sample	Elements														Ref.
	Al	**Ba**	**Ca**	**Cd**	**Co**	**Cr**	**Cu**	**Fe**	**Hf**	**I**	**K**	**Mg**	**Mn**	**Na**	
Inkjet and toner inks on paper	×	×	×	×	×	×	×	/	×	×	×	×	×	×	[46]
Inkjet ink on paper	×	×	/	×	×	/	/	×	×	×	×	/	×	×	[50]
	×	×	×	×	/	×	/	×	×	×	/	/	×	×	[51]
	/	×	/	×	×	×	×	×	×	×	/	×	×	/	[53]
Toner ink on paper	×	×	/	×	×	/	/	×	/	×	×	/	×	×	[50]
	/	×	×	×	/	×	/	/	×	/	/	/	/	/	[51]
	×	×	/	×	×	×	×	/	×	×	×	×	×	/	[52]
	×	×	/	×	×	×	×	/	×	×	/	×	/	/	[53]
Offset ink on paper	/	/	/	×	/	×	/	×	×	×	/	/	/	/	[53]
Intaglio ink on paper	/	×	/	×	/	×	/	×	×	×	/	/	/	/	[53]
Ink on pharmaceutical packages	/	/	/	/	×	/	/	/	×	×	/	/	/	×	[40]

/ indicates the presence of the element in the sample.
× indicates the element was not reported by the authors.

Table 4. List of elements detected in printed documents (continued)

Sample	Elements															Ref.
	Nb	**Ni**	**Pd**	**Rb**	**Rh**	**S**	**Sb**	**Sc**	**Si**	**Sr**	**Ti**	**V**	**Y**	**Zn**	**Zr**	
Inkjet and toner inks on paper	×	×	×	×	×	×	×	×	×	/	/	×	×	×	×	[46]
Inkjet ink on paper	×	×	×	×	×	×	×	×	/	/	×	×	×	×	×	[50]
	×	×	×	×	×	×	×	×	×	×	×	×	×	×	×	[51]
	×	×	×	×	×	×	×	×	×	×	×	×	×	×	×	[53]
Toner ink on paper	×	×	/	×	/	×	×	×	/	/	/	/	×	×	×	[50]
	×	/	×	/	×	/	/	/	/	/	/	/	/	/	/	[51]
	×	×	×	×	×	×	×	×	×	×	/	×	×	×	×	[52]
	×	×	×	×	×	×	×	×	/	×	×	×	×	×	×	[53]
Offset ink on paper	×	×	×	×	×	×	×	×	/	/	/	×	×	×	×	[53]
Intaglio ink on paper	/	×	×	×	×	×	×	×	×	/	/	×	×	×	/	[53]
Ink on pharmaceutical packages	×	/	×	×	×	×	×	×	/	/	/	×	×	×	×	[40]

/ indicates the presence of the element in the sample.
× indicates the element was not reported by the authors.

(a)

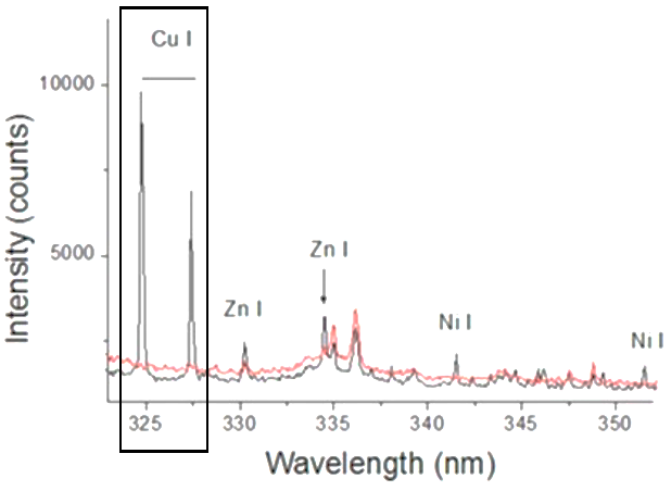

(b)

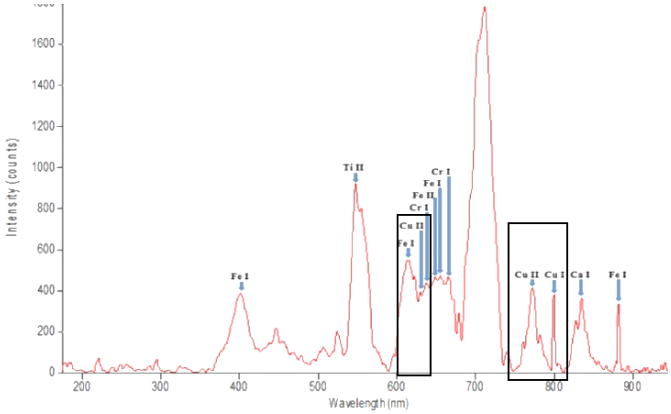

Figure 3. Presence of Cu detected in LIBS spectra of ballpoint pens by (a) Cicconi *et al*. [3] and (b) Sadam *et al*. [48]

and inkjet ink printed on paper as substrate [46, 50-53]. Only one study analyzed printing ink on pharmaceutical packages [40].

Several studies employed the conventional technique of spectral overlay as the data acquisition approach [40, 46, 51, 53]. This approach minimized errors when comparing spectral regions with no linear response and below the detection limit [51]. Two examiners independently reviewed the spectral data to discriminate between the samples based on the differences and similarities of the replicated spectra [16, 51]. The spectra were first divided into smaller regions of interest. In the LIBS software, the signals between replicates for each region were normalized with background subtraction [46, 51]. At least two spectral lines for each element beyond the detection limit were identified by employing a peak search tolerance comparable to spectra resolution [16, 46, 51]. This allows for a comparison of replicates within the samples, highlighting the variability within the samples. The samples were discriminated if any significant difference between the samples (e.g., spectral shapes and peak heights) was detected [46, 51].

Table 5 shows that LIBS detected fewer elements in inkjet ink samples than in other ink samples [8, 34, 52]. Similar elements of Ca, Mg, Cu, and K were identified in inkjet ink [50, 51, 53]. Li was detected in inkjet ink only since it is vital for electrical conductivity in inkjet printing [51, 53]. Additionally, Subedi *et al*. [53] discovered Al and Na in inkjet ink, whereas Trejos *et al*. [51] detected Co. Lennard *et al*. [50] detected Sr, Si and Cr. The chemical formulations of inkjet ink may cause fewer elements to be detected in this ink than in toner ink [53]. Furthermore, inkjet ink was partially absorbed into paper fiber. This absorption caused poor discrimination due to interferences from high paper contribution [52].

In contrast, toner ink was deposited onto the paper surface. Therefore, this ink type was discriminated efficiently [52]. A similar observation was found with a tandem LIBS-LA-ICP-MS in which inkjet ink was primarily embedded in the paper fiber while the layers of other ink types (toner, offset, and intaglio inks) were slightly raised above the paper [53]. Figure 4 shows an example of LIBS spectrum obtained from toner ink on paper with the peaks assigned to specific elements present in the samples [34, 46].

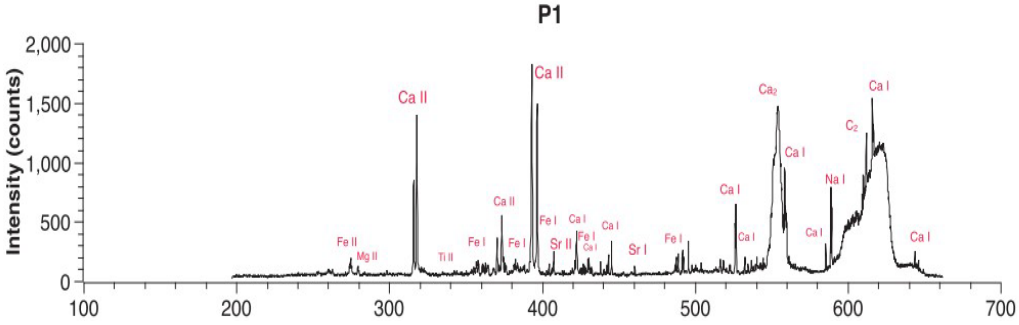

Figure 4. LIBS spectrum of toner ink sample labelled as P1 [46]

According to Lennard *et al*. [50], the selected emission lines for detected elements in toner inks were the following; Mg I (285.21 nm), Si I (288.21 nm), Rh I (332.3 nm), Hf II (325.37 nm), Ti I (498.17 nm), Sr II (460.73 nm), Cr I (520.84 nm), Ca I (643.91 nm), Cu I (327.36 nm), V I (440.82 nm), and Pd I (324.27 nm). As for Hui *et al*. [46], only several spectra regions of interest (220-278 nm, 320-360 nm, 400-420 nm, and 460-500 nm) were used to detect emission lines from ink compositions in order to reduce the contribution from paper spectra. As seen in Figure 5, both Fe II and Mg II were detected in the 220 nm to 280 nm region [46]. A minimal paper contribution was observed for Fe II, but the paper contribution was similar to the ink component for Mg II [46].

Moreover, only quantitative differences were observed for all toner ink samples except for one photocopier sample that showed qualitative differences [46]. This sample showed unique lines of Sr at wavelengths 407.41 nm, 460.73 nm, and 421.27 nm. The highest number of elements in toner inks was 20 elements, as shown by Trejos *et al*. [51], who detected Ni, Sc, I, Sb, V, Y, Rb, and S in toner ink samples that went undetected in other studies. Meanwhile, only Lennard *et al*. [50] detected Rh, Pd, and Hf. Metzinger *et al*. [52] found that most black toner ink samples had carbon-based particles or soot, but one of the samples had iron oxide. They also noted that UV spectra showed fewer lines, and their structured background had lower intensity than Vis spectra. Furthermore, the detection of Zr, Nb and Hf in toner ink samples was expected since these elements had been included in several patents and books for toner ink formulations [58, 59]. Subedi *et al*. [53] analyzed offset and intaglio inks. They postulated that each of these ink types had a single element that was absent in other ink. As for offset ink, Ba was detected whereas Nb was discovered in intaglio inks only [53].

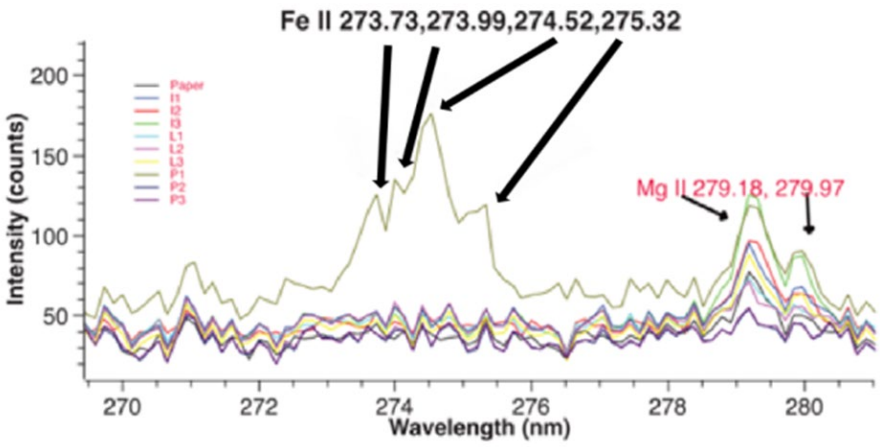

Figure 5. Emission lines of elements Fe II and Mg II in samples with paper contribution [46]

4.3 Detected elements in other types of documents

The examination of questioned documents extends beyond written or printed texts on plain paper and includes various types of documents such as identity documents, stamps, banknotes, etc. Currently, LIBS has been applied to analyze identity cards [54], passports [54], banknotes [34], and tax stamps [55], expanding its use to different types of documents. Analysis of ink on banknotes by Król *et al*. [34] proved the presence of Mn as the most frequent element. Their studies also detected Al, Ca, Na, K, Cr, Zr, and Ti. The emission lines of some of these elements are illustrated in Figure 6. Banknote paper has Ti due to the addition of titanium oxide during manufacturing.

Authentic and counterfeit banknotes have different ratios of elemental profiles [34]. Furthermore, the spectra of banknotes can be distinguished from standard office paper based on the number of lines in the spectra. A higher number of lines from neutral species, singly charged ions, and molecules were observed in the spectrum of banknotes. Based on a case study performed on several suspected Polish zloty banknotes, Król *et al*. [34] revealed that these banknotes were printed on standard office paper. The spectral differences between banknotes and office paper formed the basis on which to tell counterfeit banknotes apart from authentic banknotes. In addition, the research study showed the discrepancies between new banknotes and used banknotes. Qualitative differences were observed in the spectra of samples of both banknotes. Several used banknotes showed additional emission lines from Fe I at wavelengths from 371.965 nm to 374.942 nm, as shown in Figure 7. These peaks may arise from contamination due to contact with human skin and metallic parts of items such as pockets, wallets, and purses.

Król *et al*. [54] analyzed identity documents particularly passports and identity cards. They discovered that identity cards exhibited a lower number of elements compared to passports. Different areas on the identity cards (emblem, date of birth, and kinegram) showed similar elements of Ca, K, and Na. Al was also identified in the kinegram area, while Mg, Cr, Al, and La were identified in the emblem area. Furthermore, the study included an examination of old and new passports, revealing qualitative comparisons between these samples. Both old and new passports contained similar elements, which were Ca, Ti, Mg, K, Na, and Li [54]. Copper was present in old passports but absent in new passports. In contrast, the new passports contained the elements of V, Cr, Fe, Cd, Al, and La, which were not observed in old passports. It was also stated that Na and K were discovered in polycarbonate film covering the analyzed objects.

In a study conducted by Gonzaga *et al*. [55], they examined authentic and false tax stamps from liquor bottles. Th elements such as Ca, Na, Ti, Mg, K, and H were found in these samples. The peak intensity of Ca (at 585.75 nm) on hologram and blank paper region was responsible for distinguishing the authentic and false samples. False samples exhibited higher intensity of calcium peaks compared to authentic samples. This difference in peak intensity indicated that a special paper type was used in the production of the authentic samples, while a regular paper type was used for the false samples. This observation highlighted the potential of LIBS as a valuable tool for detecting counterfeit tax stamps and ensuring the authenticity of the stamps.

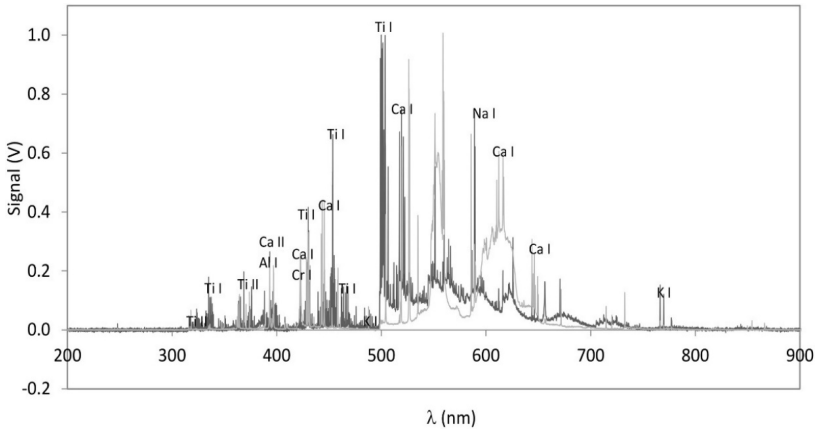

Figure 6. LIBS spectrum of a Polish banknote [34]

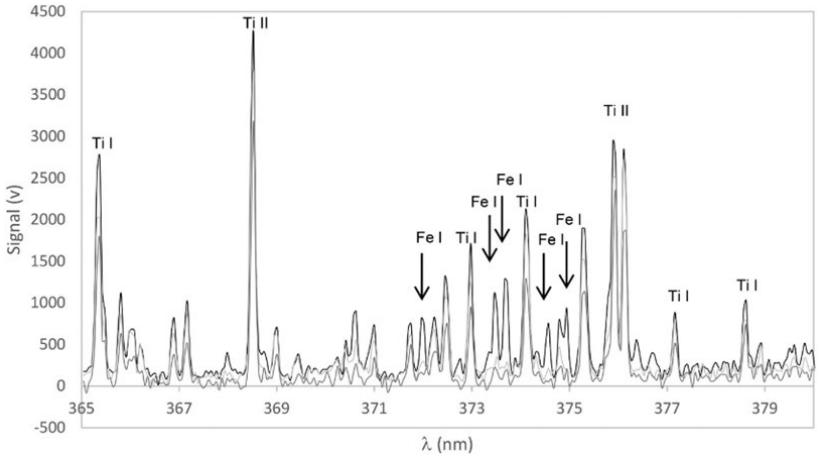

Figure 7. LIBS spectrum of used banknotes with additional lines of Fe I indicating possible contamination [34]

Another study by Haase *et al*. [40] applied LIBS to analyze printing ink on pharmaceutical packages. They observed qualitative and quantitative differences between authentic and counterfeit packages. Quantitative differences in signal intensities for peaks of K at 766 nm and Ca at 397 nm for P1 samples (authentic package) and C4 (counterfeit package) were also described. Samples P1

and C4 also showed qualitative differences with peaks of Mg (285 nm), Si (288 nm), and Al (396 nm). These elements were only found in the authentic package. As seen in Table 5, most of the detected elements (Al, Ca, Cr, Cu etc.) were similar to ink on paper except for Cd, which was detected on pharmaceutical packages only.

5. Comparison of LIBS with Other Spectroscopic Techniques

Several studies applied LIBS in conjunction with other spectroscopic instruments such as LA-ICP-MS, CE, microscopy, scanning electron microscopy – energy dispersive x-ray spectroscopy (SEM-EDS), attenuated total reflectance – Fourier transform infrared (ATR-FTIR) spectroscopy, and micro x-ray fluorescence (μXRF) analysis. The comparison of LIBS with these techniques for printing ink analysis is summarized in Table 5.

As shown in Table 5, Subedi *et al*. [53] built a tandem system of LIBS and LA-ICP-MS to analyze inkjet, toner, offset, and intaglio inks. This hybrid reduced interferences, improved discrimination ability, and provided a thorough chemical composition of printing ink. The researchers further explained that the optimization was performed differently in the standalone mode compared to the tandem mode due to different principles of the techniques. In LIBS, the excitation of atoms and ions and the correct timing for emission line acquisition are crucial for optimization. For LA-ICP-MS, the critical factors are sub-micron-sized particle production and efficient transport. LIBS optimization in tandem mode before adjusting the parameters to LA-ICP-MS were prioritized. As a result, some ICP-MS sensitivity had to be withdrawn to encourage improved performance of both methods.

Complementary information for the elements was obtained, which could not be provided by LIBS and LA-ICP-MS when used separately. LIBS detected additional elements that were used to discriminate indistinguishable samples in LA-ICP-MS. LIBS also observed fewer interferences with better signal-to-noise and reproducibility for Fe, Ca, K, and Si. Moreover, LIBS successfully detected certain elements (Si, Ca, and K) responsible for the issues in LA-ICP-MS due to isobaric interferences [51, 53]. Unlike LA-ICP-MS, LIBS could not detect all elements due to its lower sensitivity. This fact underscores the superiority of LA-ICP-MS over LIBS. Nevertheless, LIBS is an alternative method for analyzing printing ink due to its rapid speed of testing and low associated costs [51].

In terms of precision, both techniques gave comparable precision figures for inkjet ink (10%-15%). However, toner ink (3%-27%) gave poorer results due to its larger variations. Despite low repeatability between measurements, good discrimination for these inks was accomplished with both techniques. Excellent discrimination was also observed for writing inks analyzed by LA-ICP-MS with more than 95% discrimination [11]. A study by Hoehse *et al*. [7] combined LIBS with Raman spectroscopy, and the spectra from both techniques were randomly fused as previously explained. This combined approach enabled the determination of both elemental and molecular compositions of the ink samples. The data from the combined LIBS-Raman significantly enhanced the correct classifications using statistical tools, which is discussed in the following section.

SEM-EDS was applied by Trejos *et al*. [51] to analyze toner and inkjet samples. This instrument classified toner samples into sub-categories based on their iron composition. Mono-component toners contain approximately 30% to 70% of magnetite, whereas two-component toners typically lack magnetite, but they consist of up to 90% resin or binder. The latter also contains higher concentrations of surface additives (e.g., silicon). SEM-EDS was also employed to analyze gel ink pens for their morphology imaging and elemental composition [49]. SEM imaging of the ink samples revealed that the inks were absorbed into the paper fibers, making it difficult to analyze only the ink composition without some paper components. Therefore, a correction method was

Table 5. Comparison of LIBS with other techniques for document examination

Other Spectroscopic Techniques	Sample	Findings	Ref.
LA-ICP-MS	Toner, inkjet, offset, and intaglio inks on paper	• LIBS could not detect all elements found by LA-ICP-MS but LIBS detected additional elements that can discriminate indistinguishable samples in LA-ICP-MS. • LIBS could detect problematic elements (Si, Ca, and K) in LA-ICP-MS. • Lesser interferences and better signal-to-noise ratio for Fe, Ca, K, and Si in LIBS. • Both techniques showed comparable precision figures for inkjet ink (10-15%) but poorer results for toner ink (3-27%). • Tandem LIBS-LA-ICP-MS system reduced interferences and improved discrimination ability.	[51,53]
LA-ICP-MS	Ballpoint and gel ink pens	• Excellent discrimination (97.4%-99.1%) with low rates of false inclusions were obtained for the pen ink samples. • Several indistinguishable samples by LA-ICP-MS were successfully differentiated by LIBS.	[11]
SEM-EDS	Toner and inkjet inks on paper	• SEM-EDS is capable of subclassifying toner samples based on their iron composition (mono-component and two-component toners). • Sensitivity of SEM-EDS was lower compared to laser ablation methods (LA-ICP-MS and LIBS) for both inkjet and toner ink samples, resulting in relatively low discrimination (47.4% and 70.7%, respectively). • The precision results of SEM-EDS varied for different concentration levels of the element of interest (6-30% relative standard deviation).	[51]
SEM-EDS	Gel ink pens	• Both imaging and elemental analysis were performed using SEM-EDS. • SEM imaging revealed that the ink samples were absorbed into the fibers of the paper rather than forming a deposited layer on top of the paper. • The imaging analysis was also utilized to examine the morphology of the craters generated with different laser types and energies. • Similar elemental results were obtained using SEM-EDS as compared to spectra from IR and LIBS. • SEM-EDS successfully analyzed chlorine which is a difficulty for LIBS but it was incapable of analyzing Ni and Fe, which are distinguishable using LIBS.	[49]

Table 5. Comparison of LIBS with other techniques for document examination (continued)

Other Spectroscopic Techniques	Sample	Findings	Ref.
Raman spectroscopy	Blue and black ink samples	• A combination of LIBS with Raman spectroscopy improved the classification of ink samples and enhanced the correct classifications using statistical analysis. • LIBS provided elemental information of the ink samples, whereas Raman spectroscopy revealed the information on molecular composition of the samples.	[7]
ATR-FTIR spectroscopy	Ink on pharmaceutical packages	• Information from LIBS and ATR-FTIR were complementary. • LIBS provided inorganic elemental information. • ATR-FTIR revealed the presence of organic compounds.	[40]
µXRF analysis	Ink on banknotes	• Elemental compositions from LIBS and µXRF strongly varied from the same measuring area.	[34]
Microscopy analysis	Ballpoint, gel, porous point, and rollerball ink pens	• The results of analyzing pen ink samples under a microscope with IR radiation did not show any differences in the composition of the ink samples.	[2]
ICP OES	Ballpoint ink pens	• The application of cluster classification using data from ICP OES resulted in a clearer differentiation of the samples, grouping them based on the highest element content present in the samples.	[48]

required to subtract the paper spectrum. Additionally, the crater morphology produced by visible and IR lasers was observed using SEM imaging. The visible wavelength at 532 nm resulted in larger and deeper craters (~570 µm in diameter) compared to the fundamental wavelength at 1064 nm (~350 µm in diameter). Additionally, higher pulse energy with 1064 nm wavelength produced craters of comparable size, although they were still shallower than those from the visible laser.

Haase *et al*. [40] applied ATR-FTIR spectroscopy and LIBS to analyze pharmaceutical packages. They discovered that the information from ATR-FTIR spectroscopy was complementary to that from LIBS analysis. ATR-FTIR provided information of organic constituents, while LIBS revealed the presence of inorganic elements in the samples. However, several peaks from the inorganic composition appeared in ATR-FTIR spectra in the region from 1000 cm^{-1} to 400 cm^{-1}. Król *et al*. [34] compared the performance of LIBS against µXRF in the ink analysis of banknote papers. They discovered that elemental compositions from LIBS and µXRF strongly varied even in the same area of the banknote papers. The distinction between these two techniques was likely caused by the differences in penetration depth and sensitivity.

Kula *et al*. [2] highlighted that microscopic observation of pen inks was unsuccessful since no difference was detected between the samples. ICP OES was applied by Hilario *et al*. [47] to examine hand-written documents and this technique showed a more visible sample discrimination. The samples were grouped into three main elements, especially P, Cu, and Cr. Each technique listed

in Table 4 has its own strengths and limitations compared to LIBS. The advantages and disadvantages of these techniques are summarized in Table 6.

6. Merging LIBS with Multivariate Data Analysis

Multivariate data analysis or statistical analysis is the application of statistical tools combined with scientific studies to improve sample discrimination and produce extensive data. Manual processing of datasets from LIBS can be impractical due to the combined complexities and sheer volume of chemical information (sometimes more than 500 spectral lines) in the spectra, especially with many samples [33, 36, 40, 56, 60]. Chemometric analysis can be introduced to extract useful information for the systematic classification of samples based on the differences among the acquired spectra [40, 56]. This analysis is advantageous for printing ink analysis since it reveals minimal differences between ink samples with the return of higher accuracy for ink discrimination.

Chemometric analysis can be categorized into supervised and unsupervised pattern recognition techniques. Unsupervised patten recognition techniques analyze datasets without prior knowledge of classes or categories, whereas supervised techniques are used to construct training models using samples with known class or categories [56]. Principal component analysis (PCA) is an unsupervised data analysis which reduces the spatial dimensionality of the original dataset by transforming the original variables into a smaller set of independent variables called principal components (PCs) [33, 61]. PCA visualizes and interprets the variations among the variables in order to identify the similarities and differences between the samples [37, 61]. Cluster analysis (i.e., hierarchical cluster analysis or HCA) is an exploratory technique used for grouping samples based on the types of similarity measures used [62]. This technique classifies samples with similar spectral signatures and the number of clusters is determined using Ward's method as clustering algorithm and Euclidean distance as the similarity measure.

Supervised pattern recognition techniques are included in machine learning (ML) algorithms. Several ML algorithms have been employed in document examination with the application of LIBS such as *k*-nearest neighbor (KNN), linear discriminant analysis (LDA), multivariate curve resolution - alternating least square/discriminant analysis (MCR-ALS/DA), partial least squares discriminant analysis (PLS-DA), soft independent modeling of class analogy (SIMCA), support vector machine (SVM), and backpropagation (BP) neural network [1, 3, 7, 40, 52, 55]. ML can organize data into separate groups using their names, attributes, interconnections, and occurrences by disassembling and reassembling their concepts [68]. This enables powerful searches within these categories, thereby automating the sorting of data instead of relying on manual sorting. ML has the potential to be at the core of future research involving ink analysis for various documents.

KNN can be applied to classify unknown samples by calculating the nearest distance of the unknown sample to the different types of known samples [56, 61]. A training set is built in KNN prior to constructing the classification model. LDA highlights the linear separation of two data populations by maximizing the separation between the populations [61]. This model functions as a confirmation of whether the sample groups are correctly discriminated, and the unknown samples are correctly classified. The MCR method is suitable for analyzing individual data matrices and the algorithm of MCR-ALS solves the MCR basic bilinear model using a constrained alternating least squares algorithm [61]. MCR-ALS enhances the interpretability of profiles within pure spectra matrices.

Table 6. Advantages and disadvantages of different techniques used in conjunction with LIBS

Spectroscopic techniques	Advantages	Disadvantages
LA-ICP-MS	• Superior detection limits of LA-ICP-MS compared to LIBS, which are in sub-ppm levels [51, 53]. • Its high sensitivity allows for a more extensive range of trace elements and provides an excellent discrimination power [51, 53]. • LA-ICP-MS is capable of multi-elemental, micro-bulk analysis with minimal sample destruction within short period [51].	• Quadrupole mass analyzer is only capable of distinguishing ions (elements such as S, Ca, Fe, K, and halogens) with one-mass unit difference [53]. • Argon-based ICP introduces isobaric and polyatomic interferences [53]. • High cost and complexity of operation as compared to LIBS [51, 53].
SEM-EDS	• SEM-EDS is a non-destructive analysis [51]. • SEM-EDS can provide both elemental and imaging analysis [51].	• SEM-EDS exhibits low discrimination capability compared to laser-based methods (LA-ICP-MS and LIBS) due to its poor sensitivity [51]. • Acquisition time of SEM-EDS is high with around 20 min per replicate [51].
ATR-FTIR spectroscopy	• Technique of ATR-FTIR is portable, non-destructive, sensitive, and minimally invasive [40]. • Speed of analysis is only under one minute [40]. • ATR-FTIR is suited for on-site applications during real seizures or at points of care [40].	• ATR-FTIR could not detect compounds with nonpolar bonds, limiting qualitative information of the samples [63].
μXRF analysis	• μXRF requires low cost and it has high sample throughput [34]. • The operation of this method is relatively easy [34].	• Its penetration depth depends on the elemental composition, density, and absorption characteristics of the sample [34]. Thus, analysis of thin objects may be unsuitable for this method due to possible contamination from underneath the sample, resulting in misinformation.
Raman spectroscopy	• Raman spectroscopy is fast and non-destructive that requires only a small amount of samples [61]. • This technique enables direct analysis of samples with reproducible and robust results [61].	• Raman spectroscopy has low sensitivity due to naturally weak Raman scattering [64]. • Raman spectra can be interfered by intense fluorescence signals, which can obscure the chemical information of the analyzed samples [1, 64].

Table 6. Advantages and disadvantages of different techniques used in conjunction with LIBS (continued)

Spectroscopic Techniques	Advantages	Disadvantages
Microscopy analysis	• Microscopy analysis is non-invasive, which preserves the integrity of the samples [2]. • This technique's cost-effectiveness and simplicity is preferable among researchers [65].	• Microscopic method can be misleading since this approach highly depends on human interpretation and the analyst's skills [65].
ICP OES	• ICP OES is a highly sensitive technique, yielding results with excellent quality particularly in quantitative analysis [47, 66, 67].	• ICP OES requires sample digestion which can cause damage to the samples thus, this technique is less preferable for very small sample quantities [47, 66].

BP neural network is operated by propagating the signal forward and the error backward [1]. The error is determined by comparing the results obtained from each training with the expected outcomes. This algorithm adaptively adjusted its parameters to create a model that matches the characteristics of the training data. SVM is often used to model nonlinear relationships for spectral regression purposes [7]. This algorithm provides unique classification results excluding multiple classifications which leads to more precise and definitive categorization. SIMCA is primarily based on PCA in which PCA is first used to obtain PCs from sample classification [62]. The best model is developed from all types of samples and is then used for predicting the class of unknown samples. PLS-DA can be applied to first order data by obtaining a vector for each sample [69]. These vectors are organized into a matrix and PLS-DA decomposes the matrix into scores and loadings matrices in order to develop a model.

Other statistical approaches used with LIBS are analysis of variance (ANOVA), t-test, and 3-sigma criterion. ANOVA is a test that allows for simultaneous analysis of the relationship between several variables and a common set of predictors [61]. A t-test can be applied to compare the means of two sample groups that meet the requirements of normality, independence, and equal variance [70]. Two types of t-tests are widely applied for normally distributed data which are the two-sample t-test and the paired t-test [70, 71]. The 3-sigma criterion, or empirical rule, is used to determine the detection limit values within normally distributed data [70, 72, 73]. This rule states that nearly all observed data will lie within three standard deviations of the mean of the data [72]. A summary of applied statistical analyses in previous studies is shown in Table 7.

Relative standard deviation values for datasets from LIBS were higher (around 28%) compared to μXRF (around 20%) when the quantitative repeatability of these methods was taken into consideration [34]. Therefore, the repeatability of LIBS is slightly lower than μXRF. Principal component analysis (PCA) was applied for toner and inkjet ink samples. It was found that PCA offered good separation and variation (beyond 95%) between brands and models of these samples [46, 50]. Trejos *et al*. [51] noted that PCA required an extensive sampling collection. On top of the sampling requirement, it is vital to gather information from the ink manufacturers for systematic grouping of printing ink based on their brand and source.

Table 7. Application of various statistical analyses with LIBS for document examination

Statistical Analysis	Findings	Ref.
PCA	• PCA showed good differentiation and variation (beyond 95%) for toner and inkjet ink as well as gel ink pens. • PCA revealed batch-to-batch variation among ballpoint pens with similar brand and model, whereas no significant difference was observed for pens from the same box. Good discrimination was provided by PCA for different models of pens with similar brand. • As for pencil marks, PCA successfully separated all four types of samples. • PCA aided in separating false tax stamps from authentic stamps. The false stamps were also categorized into three distinct subgroups. • Large sampling collection and significant information from ink manufacturers were required for sample grouping. • PCA reduced variables prior to classifications with supervised machine learning models. • When datasets of LIBS and Raman for ink samples were used separately for PCA, LIBS data showed lesser discrimination power data from Raman. Data fusion of LIBS and Raman resulted in higher discrimination power.	[3, 4, 7, 40, 46, 47, 50, 51, 55]
HCA	• HCA exhibited similar pattern for tax stamp samples with PCA. The false and authentic stamp samples were effectively separated, with the false samples being classified into three well-defined subgroups.	[55]
ML methods	• Data fusion of LIBS and ATR-FTIR resulted in robust classification models of KNN and LDA with low error and confusion rates for ink on pharmaceutical packages. The models showed high accuracy with correct classification rates for LDA (85-99%) and KNN (90-100%). • As for ballpoint and gel pens, results of LDA showed that errors in classification may be affected by low corresponding amount of the elements used in the model, reducing the correct classification rate to 89%. • A high identification accuracy was observed for pencil marks samples (more than 96%) using KNN after reducing the data dimension with PCA, creating PCA-KNN identification model. • BP neural network was applied for pencil marks samples and high classification accuracy was observed (97.5%). The model was verified for its stability using 10-fold cross-validation. The fluctuation of the model was less than 0.04, indicating a stable model. • SIMCA successfully classified blue and black ink samples although several samples required further analysis. • SVM yielded a correct classification of 97% using fused LIBS-Raman spectra.	[2, 3, 7, 40]

Table 7. Application of various statistical analyses with LIBS for document examination (continued)

Statistical Analysis	Findings	Ref.
Discriminant analysis	• Advanced multivariate statistical analysis and results of high accuracy and reliability were accomplished with MCR-ALS/DA. UV range (83%) presented better results compared to Vis (60%) and UV-Vis (71%) ranges for print identifications. • PLS-DA models of tax stamp samples were 100% accurate in identifying and classifying authentic and false samples with no classification error. • PLS-DA model created using fused LIBS-Raman spectra effectively classified all blue and black ink samples.	[52, 55]
ANOVA	• Analysis of Variance (ANOVA) with Tukey's post hoc test produced excellent discrimination for toner (98%) and inkjet (100%) samples. • Similar approach was employed for gel ink pens, obtaining non-significant results for similar brands, manufacturers, and batches but highly significant differences were observed among different samples ($p = 0.0001$). • Tukey's post hoc test at a 95% confidence limit determined which gel ink pen was responsible for the differences or the unique effect. • ANOVA was applied with 3-sigma rule, yielding excellent discrimination for black (99%) and blue (100%) ballpoint pens.	[4, 50]
3-sigma criterion	• Excellent discrimination was achieved for toner ink samples (97%) and inkjet ink samples (93%). • 3-sigma rule was employed with ANOVA, which successfully discriminated black and blue ballpoint pens.	[50]
t-test	• t-test with a 95% confidence limit discriminated three indistinguishable pairs of toner samples and nine indistinguishable pairs of ballpoint pens with 99.8% discrimination.	[50]

Haase *et al*. [40] implemented PCA prior to classifications with supervised ML models of KNN and LDA. PCA reduced the variables to be used as data input for these classifiers. The classifications with KNN and LDA were realized by combining the data from LIBS and ATR-FTIR. The hybrid data produced robust classification models with low error and confusion rates. These models had high accuracy, as observed in the classification rate for both LDA (85%-99%) and KNN (90%-100%). In contrast to models from separate datasets, lower percentages were observed in LIBS datasets, with 69% to 94% for LDA and 74% to 97% for KNN. ATR-FTIR datasets gave outputs of 81% to 95% and 88% to 99% for KNN and LDA, respectively. Data fusion of LIBS and Raman also improved the classification of the samples using ML models of SVM and SIMCA [7]. The fusion combined the benefits of both LIBS and Raman techniques resulting in higher discrimination power.

In a study conducted by Lennard *et al*. [50], high discrimination was achieved for both toner and inkjet ink samples using the 3-sigma criterion. They reported that the inkjet samples exhibited 93% discrimination (with one indistinguishable pair), while the toner samples showed 97% discrimination (with five indistinguishable pairs). The 3-sigma rule was chosen over the 2-sigma rule due to the low standard deviation between replicates for ink samples [50]. Moreover, excellent results were observed in the application of ANOVA with Tukey's post hoc test for toner samples (98% discrimination with three indistinguishable pairs) and inkjet ink samples (100% discrimination) [50]. For the three indistinguishable pairs of toner samples, the researchers used a student t-test at a 95% confidence limit for discrimination [50]. A similar approach utilizing the 3-sigma rule with ANOVA was employed for pen inks, resulting in 99% discrimination for black pens and 100% for blue pens [50]. Likewise, the researchers subjected the indistinguishable pairs of pen inks to a student t-test which discriminated seven out of nine pairs, yielding a discrimination power of 99.8%.

In addition, the MCR-ALS/DA approach produced accurate results for print identifications, and superior results were observed in the UV range compared to the Vis and UV-Vis ranges [52]. The UV range showed the highest accuracy with 40 out of 48 correct identifications (83%). As for the rest of the spectral ranges, the Vis range had an accuracy of 60%, while the UV-Vis range was accurate by 71% for print identifications. The UV range showed low spectral background and the number of peaks resulting in highly distinctive spectral features. Therefore, better results were observed in the MCR-ALS/DA approach by using the UV range.

Al-Ameri *et al*. [45] proposed an unsupervised clustering algorithm inspired by the DBSCAN algorithm (density-based spatial clustering of applications with noise). Their research primarily focused on developing the algorithm and they did not provide details on the elemental profiles of the samples in their study. Although the same steps for the DBSCAN algorithm were followed, they adopted a different approach. The proposed algorithm successfully distinguished forged toner ink on questioned documents from original toner ink with 92.08% accuracy. Moreover, toner and inkjet inks were correctly classified into their respective clusters. It was highlighted that the proposed algorithm is cheap, easy to implement, non-destructive, and visually interpretable. However, they acknowledged certain limitations such as the requirement for the laser in LIBS system to have high stability to ensure even energy distribution in each pulse, and any change in LIBS system affects the accuracy of the proposed algorithm.

Although chemometric tools allow for easy data processing, there are several limitations for certain statistical tests when analyzing data [33]. Improper utilization of statistical software and algorithm can lead to the enhancement of poor characterization by high fluctuations and low sensitivity. The advantages and disadvantages of statistical analyses are listed in Table 8. Despite the limitations listed in Table 8, these statistical analyses can reliably classify, discriminate, and group chemical datasets [66]. Furthermore, the discriminating power of analytical methods including LIBS can be increased to improve data interpretation and presentation.

Table 8. Advantages and disadvantages of statistical analyses applied for document examination

Advantages	Disadvantages
• PCA can clearly separate data points for sample classification based on characteristic LIBS spectra [33]. • ML algorithms often produce excellent results [39]. • Procedure of the 3-sigma criterion can easily compute the detection limits of a dataset [73]. • BP neural network is capable of processing large amounts of data with remarkable optimization and convergence speed thus, the whole wavelength range can be used for the analysis [1]. • BP neural network can accurately obtain recognition results [1]. • Calculation time of SVM is usually a few seconds faster compared to PCA and SIMCA [7].	• Discriminatory capability of PCA can be overwhelming when there are substantial differences in the data, diminishing the smaller differences among the remaining data [33]. • ML algorithm requires an extensive training dataset, and it necessitates time for classification due to high-dimensional data [1, 39]. • The rate of false negatives can be quite high when applying 3-sigma rule due to the limited amount of variability, resulting in a low value of the 3-sigma rule [73]. • The first result of BP neural network is often poor since the model requires feedback to optimize itself for data processing [1]. • Visualization of the identification process using BP neural network is difficult [1]. • SIMCA requires a long time for calculation depending on the size of the dataset [7] and it tends to yield poor results when the differences between classes are small [67].

7. Conclusions

The application of spectroscopic techniques, including LIBS, has garnered attention among document examiners. This review article discussed the strengths and limitations of LIBS as an alternative technique in ink analysis. Although the applications of LIBS are still relatively new in document examination, several peer-reviewed studies have demonstrated its reliability in qualitatively and quantitatively distinguishing ink samples on various substrates. LIBS provides crucial information on ink samples, corroborating the results obtained from other analytical methods and overcoming their limitations (e.g., LA-ICP-MS, ATR-FTIR, and μXRF). Furthermore, LIBS demonstrated excellent results when coupled with statistical analysis in achieving higher accuracy for ink discrimination. Future research endeavors may delve into the combination of LIBS with spectroscopic and statistical methods that have yet to be investigated. Additionally, there is potential for the use of LIBS to analyze various other types of writing instruments and printing machines to enhance the scope of LIBS application in this field.

8. Acknowledgements

The authors would like to express their gratitude to the Universiti Teknologi MARA, Malaysia for funding under the Geran Insentif Penyeliaan (600-RMC/GIP 5/3 (087/2021)) as well as individuals who contributed to the content of this review paper.

References

[1] Chen, Y., Liu, Y., Han, B., Yu, W. and Wan, E., 2022. Identification of writing marks from pencil lead through machine learning based on laser-induced breakdown spectroscopy. *Optik*, 259, https://doi.org/10.1016/j.ijleo.2022.169008.

[2] Kula, A., Wietecha-Posłuszny, R., Pasionek, K., Król, M., Woźniakiewicz, M. and Kościelniak, P., 2014. Application of laser induced breakdown spectroscopy to examination of writing inks for forensic purposes. *Science and Justice*, 54(2), 118-125, https://doi.org/10.1016/j.scijus.2013.09.008.

[3] Cicconi, F., Lazic, V., Palucci, A., Assis, A.C.A. and Romolo, F.S., 2020. Forensic analysis of commercial inks by laser-induced breakdown spectroscopy (LIBS). *Sensors*, 20(13), https://doi.org/10.3390/s20133744.

[4] Balah, O.F.A. and Nassef, O.A.T., 2019. A further analysis of laser-induced breakdown spectroscopy ink pens' spectra using principal component analysis (PCA) for forensic characterization. *Arab Journal of Nuclear Sciences and Applications*, 52(2), 72-78, https://doi.org/10.21608/ajnsa.2019.4231.1097.

[5] Reed, G., Savage, K., Edwards, D. and Daeid, N.N., 2014. Hyperspectral imaging of gel pen inks: An emerging tool in document analysis. *Science and Justice*, 54(1), 71-80, https://doi.org/10.1016/j.scijus.2013.09.005.

[6] Hark, R.R. and East, L.J., 2014. Forensic applications of LIBS. In: S. Musazzi and U. Perini, eds. *Springer Series in Optical Sciences*. Berlin: Springer, pp. 377-420.

[7] Hoehse, M., Paul, A., Gornushkin, I. and Panne, U., 2012. Multivariate classification of pigments and inks using combined Raman spectroscopy and LIBS. *Analytical and Bioanalytical Chemistry*, 402(4), 1443-1450, https://doi.org/10.1007/s00216-011-5287-6.

[8] Shaffer, D.K., 2009. Forensic document analysis using scanning microscopy. *Proceedings of the SPIE*, 7378, https://doi.org/10.1117/12.825186.

[9] Calcerrada, M. and García-Ruiz, C., 2015. Analysis of questioned documents: A review. *Analytica Chimica Acta*, 853(1), 143-166, https://doi.org/10.1016/j.aca.2014.10.057.

[10] Poon, N.L., Ho, S.S.H. and Li, C.K., 2005. Differentiation of coloured inks of inkjet printer cartridges by thin layer chromatography and high performance liquid chromatography. *Science and Justice*, 45(4), 187-194, https://doi.org/10.1016/S1355-0306(05)71665-8.

[11] Trejos, T., Flores, A. and Almirall, J.R., 2010. Micro-spectrochemical analysis of document paper and gel inks by laser ablation inductively coupled plasma mass spectrometry and laser induced breakdown spectroscopy. *Spectrochimica Acta Part B: Atomic Spectroscopy*, 65(11), 884-895, https://doi.org/10.1016/j.sab.2010.08.004.

[12] Szafarska, M., Wietecha-Posłuszny, R., Woźniakiewicz, M. and Kościelniak, P., 2011. Examination of colour inkjet printing inks by capillary electrophoresis. *Talanta*, 84(5), 1234-1243, https://doi.org/10.1016/j.talanta.2010.12.024.

[13] Król, M., Kula, A., Wietecha-Posłuszny, R., Woźniakiewicz, M. and Kościelniak, P., 2012. Examination of black inkjet printing inks by capillary electrophoresis. *Talanta*, 96, 236-242, https://doi.org/10.1016/j.talanta.2011.12.025.

[14] Lee, J., Nam, Y.S., Min, J., Lee, K.B. and Lee, Y., 2016. TOF-SIMS analysis of red color inks of writing and printing tools on questioned documents. *Journal of Forensic Sciences*, 61(3), 815-822, https://doi.org/10.1111/1556-4029.13047.

[15] Materazzi, S., Risoluti, R., Pinci, S. and Romolo, F.S., 2017. New insights in forensic chemistry: NIR/Chemometrics analysis of toners for questioned documents examination. *Talanta*, 174, 673-678, https://doi.org/10.1016/j.talanta.2017.06.044.

[16] Trejos, T., Torrione, P., Corzo, R., Raeva, A., Subedi, K., Williamson, R., Yoo, J. and Almirall, J., 2016. A novel forensic tool for the characterization and comparison of printing ink evidence: Development and evaluation of a searchable database using data fusion of spectrochemical methods. *Journal of Forensic Sciences*, 61(3), 715-724, https://doi.org/10.1111/1556-4029.13109.

[17] Sharaa, S.I., Elmagd, A.A.S.A., Bakr, A.-S.A., Moustafa, Y.M., Shabana, A.A. and El-Aziz, I.A., 2019. The physical application of non-destructive techniques in detection the sequence of intersecting gel ink and printed laser toner strokes. *Egyptian Journal of Chemistry*, 62(6), 1469-1491, https://doi.org/10.21608/EJCHEM.2019.6532.1549.

[18] Verma, N., Kumar, R. and Sharma, V., 2018. Analysis of laser printer and photocopier toners by spectral properties and chemometrics. *Spectrochimica Acta Part A: Molecular and Biomolecular Spectroscopy*, 196, 40-48, https://doi.org/10.1016/j.saa.2018.02.001.

[19] Verma, N., Sharma, V., Kumar, R., Sharma, R., Joshi, M.C., Umapathy, G.R., Ohja, S. and Chopra, S., 2019. On the spectroscopic examination of printed documents by using a field emission scanning electron microscope with energy-dispersive X-ray spectroscopy (FE-SEM-EDS) and chemometric methods: application in forensic science. *Analytical and Bioanalytical Chemistry*, 411(16), 3477-3495, https://doi.org/10.1007/s00216-019-01824-z.

[20] Brech, F. and Cross, L., 1962. Optical microemission stimulated by a ruby laser. *Applied Spectroscopy*, 16(2), 59-64.

[21] Kaiser, J., Novotný, K., Martin, M.Z., Hrdlička, A., Malina, R., Hartl, M. and Kizek, R., 2012. Trace elemental analysis by laser-induced breakdown spectroscopy—biological applications. *Surface Science Reports,* 67(11-12), 233-243.

[22] Rehse, S.J., Salimnia, H. and Miziolek, A.W., 2012. Laser-induced breakdown spectroscopy (LIBS): an overview of recent progress and future potential for biomedical applications. *Journal of Medical Engineering and Technology,* 36(2), 77-89.

[23] Santos, D.J., Nunes, L.C., de Carvalho, G.G.A., Gomes, M.D.S., de Souza, P.F., Leme, F.D.O. and Krug, F.J., 2012. Laser-induced breakdown spectroscopy for analysis of plant materials: a review. *Spectrochimica Acta Part B: Atomic Spectroscopy,* 71-72, 3-13.

[24] Pořízka, P., Prochazková, P., Prochazka, D., Sládková, L., Novotný, J., Petrilak, M. and Kaiser, J., 2014. Algal biomass analysis by laser-based analytical techniques—a review. *Sensors,* 14(12), 17725-17752.

[25] Harmon, R.S., Russo, R.E. and Hark, R.R., 2013. Applications of laser-induced breakdown spectroscopy for geochemical and environmental analysis: a comprehensive review. *Spectrochimica Acta Part B: Atomic Spectroscopy,* 87, 11-26.

[26] Corsi, M., Cristoforetti, G., Hidalgo, M., Legnaioli, S., Palleschi, V., Salvetti, A., Tognoni, E. and Allebona, C., 2003. Application of laser-induced breakdown spectroscopy technique to hair tissue mineral analysis. *Applied Optics,* 42, 6133-6137.

[27] Ahmed, H.E. and Nassef, O.A., 2013. From Ptolemaic to modern inked linen via laser induced breakdown spectroscopy (LIBS). *Analytical Methods,* 5, 3114-3121.

[28] Ponterio, R., Trusso, S., Vasi, C., La Torre, G.F. and Raffa, A.T., 2008. Laser induced breakdown spectroscopy for the analysis of archaeological dyes from Licata (Sicily). *Radiation Effects and Defects in Solids,* 163(4-6), 535-543.

[29] Noll, R., 2012. *Laser-induced Breakdown Spectroscopy Fundamentals and Applications*. Berlin: Springer.

[30] Yun, J.I., Klenze, R. and Jae-Il, K., 2002. Laser-induced breakdown spectroscopy for the on-line multielement analysis of highly radioactive glass melt. Part I: Characterization and evaluation of the method. *Applied Spectroscopy,* 56(4), 437-448.
[31] Oujja, M., Vila, A., Rebollar, E., García, J.F. and Castillejo, M., 2005. Identification of inks and structural characterization of contemporary artistic prints by laser-induced breakdown spectroscopy. *Spectrochimica Acta Part B: Atomic Spectroscopy*, 60(7-8), 1140-1148, https://doi.org/10.1016/j.sab.2005.05.021.
[32] Mateo, M.P., Ctvrtnickova, T. and Nicolas, G., 2009. Characterization of pigments used in painting by means of laser-induced plasma and attenuated total reflectance FTIR spectroscopy. *Applied Surface Sciences*, 255, 5172-5176.
[33] Pořízka, P., Klus, J., Képe, E., Prochazka, D., Hahn, D.W. and Kaiser, J., 2018. On the utilization of principal component analysis in laser-induced breakdown spectroscopy data analysis, a review. *Spectrochimica Acta Part B: Atomic Spectroscopy* 148, 65-82, https://doi.org/10.1016/j.sab.2018.05.030.
[34] Król, M., Gondko, K., Kula, A., Własiuk, P., del Hoyo-Meléndez, J.M. and Kościelniak, P., 2020. Characterization of the elemental composition of Polish banknotes by X-ray fluorescence and laser-induced breakdown spectroscopy. *Spectrochimica Acta Part B: Atomic Spectroscopy*, 169, https://doi.org/10.1016/j.sab.2020.105898.
[35] Almirall, J., 2017. *Laser Ablation Inductively Coupled Plasma Mass Spectrometry (LA-ICP-MS) and Laser Induced Breakdown Spectroscopy (LIBS) Analyses of Paper, Inks, and Soils*. [online] Available at: https://www.ojp.gov/pdffiles1/nij/grants/250537.pdf.
[36] Zhang, T., Tang, H. and Li, H., 2018. Chemometrics in laser-induced breakdown spectroscopy. *Journal of Chemometrics*, 32(11), https://doi.org/10.1002/cem.2983.
[37] Spizzichino, V. and Fantoni, R., 2014. Laser induced breakdown spectroscopy in archeometry: A review of its application and future perspectives. *Spectrochimica Acta Part B: Atomic Spectroscopy*, 99, 201-209, https://doi.org/10.1016/j.sab.2014.07.003.
[38] Ikezawa, S., Wakamatsu, M., Pawlat, J. and Ueda, T., 2011. Multi-spectral analytical systems using LIBS and LII techniques. In: S.C. Mukhopadhyay, A. Lay-Ekuakille and A. Fuchs, eds. *New Developments and Applications in Sensing Technology*. Berlin: Springer, pp. 207-232.
[39] Anabitarte, F., Cobo, A. and Lopez-Higuera, J.M., 2012. Laser-induced breakdown spectroscopy: Fundamentals, applications, and challenges. *ISRN Spectroscopy*, 2012, https://doi.org/10.5402/2012/285240.
[40] Haase, E., Arroyo, L. and Trejos, T., 2020. Classification of printing inks in pharmaceutical packages by laser-induced breakdown spectroscopy and attenuated total reflectance-fourier transform infrared spectroscopy. *Spectrochimica Acta Part B: Atomic Spectroscopy*, 172, https://doi.org/10.1016/j.sab.2020.105963.
[41] Elsherbiny, N. and Nassef, O.A., 2015. Wavelength dependence of laser induced breakdown spectroscopy (LIBS) on questioned document investigation. *Science and Justice*, 55(4), 254-263, https://doi.org/10.1016/j.scijus.2015.02.002.
[42] Wei, J., Zhang, T., Dong, J., Sheng, L., Tang, H., Yang, X. and Li, H., 2015. Quantitative determination of Cr in ink by laser-induced breakdown spectroscopy (LIBS) using ZnO as adsorbent. *Chemical Research in Chinese Universities,* 31, 909-913, https://doi.org/10.1007/s40242-015-5210-3.
[43] Pollock, D. and Coulon, R., 1996. Life cycle assessment of an inkjet print cartridge. *Proceedings of the 1996 IEEE International Symposium on Electronics and the Environment*, Texas, USA, May 6-8, 1996, pp.154-160.
[44] National Institute of Standards and Technology, 2023. *National Institute of Standards and Technology*. [online] Available at: https://www.nist.gov/.

[45] Al-Ameri, M.A., Ciylan, B. and Mahmood, B., 2022. Spectral data analysis for forgery detection in official documents: A network-based approach. *Electronics*, 11(23), https://doi.org/10.3390/electronics11234036.
[46] Hui, Y.W., Mahat, N.A., Ismail, D. and Ibrahim, R.K.R., 2019. Laser-induced breakdown spectroscopy (LIBS) for printing ink analysis coupled with principle component analysis (PCA). *AIP Conference Proceedings*, 2155(1), https://doi.org/10.1063/1.5125514.
[47] Hoehse, M., Mory, D., Florek, S., Weritz, F., Gornushkin, I. and Panne, U., 2009. A combined laser-induced breakdown and Raman spectroscopy Echelle system for elemental and molecular microanalysis. *Spectrochimica Acta Part B: Atomic Spectroscopy*, 64(11-12), 1219-1227, https://doi.org/10.1016/j.sab.2009.09.004.
[48] Hilario, F.F., Lima de Mello, M. and Pereira-Filho, R., 2021. Forensic analysis of hand-written documents using laser-induced breakdown spectroscopy (LIBS) and chemometrics. *Analytical Methods*, 13(2), 232-241, https://doi.org/10.1039/d0ay02089c.
[49] Sadam, H.S., Habana, S.A. and Ali, A.H., 2019. Optimize of LIBS setup to the determination of laser breakdown power of writing inks. *Chemical and Process Engineering Research*, 61(24), 24-34, https://doi.org/10.7176/cper/61-05.
[50] Lennard, C., El-Deftar, M.M. and Robertson, J., 2015. Forensic application of laser induced breakdown spectroscopy for the discrimination of questioned documents. *Forensic Science International*, 254, 68-79, https://doi.org/10.1016/j.forsciint.2015.07.003.
[51] Trejos, T., Corzo, R., Subedi, K. and Almirall, J., 2014. Characterization of toners and inkjets by laser ablation spectrochemical methods and scanning electron microscopy-energy dispersive x-ray spectroscopy. *Spectrochimica Acta Part B: Atomic Spectroscopy*, 92, 9-22, https://doi.org/10.1016/j.sab.2013.11.004.
[52] Metzinger, A., Rajkó, R. and Galbács, G., 2014. Discrimination of paper and print types based on their laser induced breakdown spectra. *Spectrochimica Acta Part B: Atomic Spectroscopy*, 94-95, 48-57, https://doi.org/10.1016/j.sab.2014.03.006.
[53] Subedi, K., Trejos, T. and Almirall, J., 2015. Forensic analysis of printing inks using tandem laser induced breakdown spectroscopy and laser ablation inductively coupled plasma mass spectrometry. *Spectrochimica Acta Part B: Atomic Spectroscopy*, 103-104, 76-83, https://doi.org/10.1016/j.sab.2014.11.011.
[54] Król, M., Kowalska, D. and Kościelniak, P., 2017. Examination of Polish identity documents by laser induced breakdown spectroscopy. *Analytical Letters*, 51(10), 1592-1604, https://doi.org/10.1080/00032719.2017.1384833.
[55] Gonzaga, F.B., Rocha, W.F.D.C. and Correa, D.N., 2015. Discrimination between authentic and false tax stamps from liquor bottles using laser-induced breakdown spectroscopy and chemometrics. *Spectrochimica Acta Part B*, 109, 24-30, https://doi.org/10.1016/j.sab.2015.04.011.
[56] Tian-long, Z., Shan, W.U., Hong-sheng, T., Kang, W., Yi-xiang, D. and Hua, L.I., 2015. Progress of chemometrics in laser-induced breakdown spectroscopy analysis. *Chinese Journal of Analytical Chemistry*, 43(6), 939-948, https://doi.org/10.1016/S1872-2040(15)60832-5.
[57] Martinez-Lopez, C., Sakayanagi, M. and Almirall, J. R., 2018. Elemental analysis of packaging tapes by LA-ICP-MS and LIBS. *Forensic Chemistry*, 8, 40-48, https://doi.org/10.1016/j.forc.2018.01.004.
[58] U.S. Geological Survey, 2011. *Minerals Yearbook. Metals and Minerals 2008. Vol. 1.* Washinton: U.S. Government Printing Office.
[59] Iftime, G., Vanbesien, D.W., Birau, M.M., Wosnick, J.H., Kazmaier, P.M., 2013. *Toner Containing Fluorescent Nanoparticles*, USA. Patent No. 8,541,154 B2.
[60] Rzecki, K., Sośnicki, T., Baran, M., Niedźwiecki, M., Król, M., Łojewski, T., Acharya, U.R., Yildirim, Ö. and Pławiak, P., 2018. Application of computational intelligence methods for the automated identification of paper-ink samples based on LIBS. *Sensors*, 18(11), https://doi.org/10.3390/s18113670.

[61] Gorziza, R., González, M., de Carvalho, C.M.B., Ortiz, R.S., Ferrão, M.F. and Limberger, R.P., 2021. Chemometric approaches in questioned documents. *Brazillian Journal of Analytical Chemistry*, 9(34), 35-51, https://doi.org/10.30744/brjac.2179-3425.RV-32-2021.
[62] Kumar, R. and Sharma, V., 2018. Chemometrics in forensic science. *Trends in Analytical Chemistry*, 105, 191-201, https://doi.org/10.1016/j.trac.2018.05.010.
[63] Khofar, P.N.A., Karim, U.K.A., Elias, E., Safian, M.F. and Halim, M.I.A., 2022. Trends of forensic analysis of pen ink using attenuated total reflectance fourier transform infrared (ATR-FTIR) spectroscopy. *Indonesian Journal of Chemistry*, 22(4), 1144-1154. https://doi.org/10.22146/ijc.72282.
[64] Braz, A., López-López, M. and Gárcia-Ruiz, C., 2013. Raman spectroscopy for forensic analysis of inks in questioned documents. *Forensic Science International*, 232, 206-212, https://doi.org/10.1016/j.forsciint.2013.07.017.
[65] Sharaa, S.I., Elmagd, A.A.S.A., Bakr, A.-S.A., Moustafa, Y.M., El-Aziz, I.M.A. and Shabana, A., 2019. Some of the physical and chemical characterizations applied for the laser printers toner and ballpoint pen inks to determine the sequence of their intersections. *Egyptian Journal of Chemistry*, 62(11), 2047-2060. https://doi.org/10.21608/EJCHEM.2019.10960.1702.
[66] Claverie, F., 2020. Laser ablation. In: D. Beauchemin, ed. *Sample Introduction Systems in ICPMS and ICPOES*. Amsterdam: Elsevier, pp. 469-531.
[67] Rinke-Kneapler, C.N. and Sigman, M.E., 2014. Applications of laser spectroscopy in forensic science. In: M. Baudelet, ed. *Laser Spectroscopy for Sensing: Fundamentals, Techniques and Applications*. Cambridge: Woodhead Publishing Limited, pp. 461-495.
[68] Montasari, R., Carroll, F., Macdonald, S., Jahankhani, H., Hosseinian-Far, A. and Daneshkhah, A., 2020. Application of artificial intelligence and machine learning in producing actionable cyber threat intelligence. In: R. Montasari, H. Jahankhani, R. Hill. and S. Parkinson, eds. *Digital Forensic Investigation of Internet of Things (IOT) Devices*. Cham: Springer, pp. 47-64.
[69] Valderrama, L. and Valderrama, P., 2016. Nondestructive identification of blue pen inks for documentoscopy purpose using iPhone and digital image analysis including an approach for interval confidence estimation in PLS-DA models validation. *Chemometrics and Intelligent Laboratory Systems*, 156, 188-195, https://doi.org/10.1016/j.chemolab.2016.06.009.
[70] Kim, T.K., 2015. T test as a parametric statistic. *Korean Journal of Anesthesiology*, 68(6), 540-546, http://dx.doi.org/10.4097/kjae.2015.68.6.540.
[71] Xu, M., Fralick, D., Zheng, J.Z., Wang, B., Tu, X.M. and Feng, C., 2017. The differences and similarities between two-sample t-test and paired t-test. *Shanghai Archives of Psychiatry*, 29(3), 184-188, https://doi.org/10.11919/j.issn.1002-0829.217070.
[72] Hayes, A., 2023. *Empirical Rule: Definition, Formula, Example, How It's Used*, [online] Available at: https://www.investopedia.com/terms/e/empirical-rule.asp.
[73] Coleman, D. and Vanatta, L., 2008. *Statistics in Analytical Chemistry: Part 32-Detection Limits Via 3-Sigma*, [online] Available at: https://www.americanlaboratory.com/914-Application-Notes/1104-Part-32.